

Characteristics of turbulent premixed oxy-fuel combustion - A DNS study

Z J Peng¹, S H Zhong² and F Zhang^{2,3}

¹Faculty of Creative Arts, Technologies and Science, University of Bedfordshire, UK

²State Key Lab of Engines, Tianjin University, Tianjin, China

E-mail: fanzhang_lund@tju.edu.cn

Abstract. A 3D DNS numerical study with detail chemistry mechanism has been carried out to investigate turbulent premixed combustion with oxyfuel mixtures under similar operating conditions as happened in spark ignition Internal Combustion Engine (ICE). H₂O and CO₂ are adopted as the dilution in oxy-fuel combustion. The temperature profiles of oxy-H₂O and oxy-CO₂ combustion are consistent with those of air-fired conditions in laminar premixed flame when the molar fraction of H₂O and CO₂ are 73% and 66% in oxidizer, respectively. 79%, 67% molar fraction of H₂O and 79%, 56% molar fraction of CO₂ are also conducted to learn the effects of the dilution molar fraction on the process of flame propagation. With the molar fraction of dilution increases, the mass of C₂H₂ increases the flame propagation speed and the mass of CO does an opposite influence. With the investigation for effects of turbulent intensity under conditions of 73% H₂O and 66% CO₂ with the initial u' of 0.8, 1.6 and 2.4 m/s, respectively, results show that the turbulent intensity has little effect on the formation of CO. It is also demonstrated that for oxy-fuel combustion, due to the disparity in laminar flame speed, an appropriate u' is necessary to keep consistent with the flame propagation speed meanwhile to maintain suitable temperature profiles.

Nomenclature

CCS	carbon capture and storage
FDS	flame displacement speed
ICE	internal combustion engine
TDC	top dead centre
DNS	direct numerical simulation
HRR	heat release rate
PDF	probability density function

1. Introduction

Oxy-fuel combustion has attracted much attention as a promising approach to reduce CO₂ emissions by Carbon Capture and Storage (CCS) [1,2]. Compared to the traditional air/fuel combustion, oxy-fuel combustion is also a technology to achieve zero emissions of NO_x because N₂ in air is replaced generally by CO₂, H₂O (water steam) or both. It presents a practical approach to achieve more environmental-friendly gas turbines and Internal Combustion Engines (ICEs) with clean combustion [3].

However there still a lot of challenges for applying oxy-fuel combustion into practical powerplants or powertrain systems. Currently, two main barriers in this respect are: (1) the mechanical difficulty and



system control to introduce oxy-fuel combustion into current powerplants and (2) the reduced thermal efficiency due to high level energy consumption in the process of exhaust gas after-treatment and consequent CCS processes. The former one is difficult to overcome since the thermodynamic and chemical properties of the dilution directly affect combustion process, while the environmentalists pay high attention on the latter one as it is concerned the green gas control and the air pollution. It has been suggested that with the impurities of the CO₂-water-stream would increase more energy consumed to separate CO₂ from exhaust gas [4]. The impurities of CO₂-water-steam generally is due to redundant O₂ due to the incomplete combustion and some unremoved N₂ during O₂ production from air. Generally, it is more helpful for saving oxygen supply by operating oxy-fuel combustion with the equivalent ratio as 1.0. More researches for exploring characteristics of oxy-fuel combustion in gas turbines have been carried out. For instance, Liu found that if the mixture's air fuel ratio is proper, it easily resulted in the combustion flame unstable. Between the combustion flame instability and peak flame temperature, there exists a trade-off [5]. Krieger investigated the propane/oxy-fuel and syngas/oxy-fuel flame stability as a swirl diffusion flames using a simplified model [6].

With those investigation taken for the practical application of oxy-fuel combustion, it has been demonstrated that the combustion performances are largely influenced by the dilution which is provided by CO₂ or H₂O [7-10]. Because they have higher heat capacity than N₂, as shown in Table 1, gas-fuel ratio with CO₂ or H₂O as diluent should be kept lower for similar combustion characteristics compared to air-fire condition. As most of previous studies are mainly focused on laminar combustion flame conditions, characteristics of oxy-fuel combustion under turbulence combustion conditions lack adequate investigation, although actual oxy-fuel combustion is mainly under turbulent conditions.

Table 1. Physicochemical properties of relevant gases at 1000 K, 0.1 MPa

Gas	Density (mol/m ³)	C _v (J/mol·K)	C _p (J/mol·K)	Therm.Cond. (W/m·K)	ρC _p (J/m ³ ·K)	Therm.Diff (m ² /s)
H ₂ O	12.03	32.963	41.293	0.097085	496.754	0.000195
CO ₂	12.025	46	54.322	0.070571	653.222	0.000108
N ₂	12.023	24.386	32.703	0.065991	393.188	0.000168

In this study, a premixed turbulent oxy-fuel combustion in a constant vessel is simulated using DNS method, the initial conditions are simulated as similar in a conventional spark ignition Internal Combustion Engine (ICE). The pressure, temperature, Heat Release Rate (HRR), flame propagation speed and emissions are investigated under different molar fraction of dilution and turbulent intensity.

2. Initial conditions and numerical methods

2.1. Temperature Profiles Matching

In order to fit current powerplant, the temperature profile is normally used to evaluate the similarity between oxy-fuel combustion and air-fuel combustion condition. The process of temperature match is performed in CHEMKIN, using the laminar premixed flame module. Figure 1 is shown the temperature profiles of 0.71, 0.73, 0.75 and 0.77 molar fraction of H₂O in oxidizer while figure 2 represents those of 0.62, 0.64, 0.66 and 0.68 molar fraction of CO₂ in oxidizer, which are the most similar to those of air-fired condition. The fresh gas temperature is 773 K and the pressure is keep to 1 MPa. The temperature derivation σ is adopted to evaluate the similarity according to Song and Zou's work [7,8], and is calculated:

$$\sigma = \sqrt{\frac{\sum_{i=1}^N (T_{s,i} - T_{a,i})^2}{N}} \quad (1)$$

Here $T_{s,i}$ and $T_{a,i}$ represent the temperature values of node i during oxy-fuel combustion and air-fired

condition, respectively.

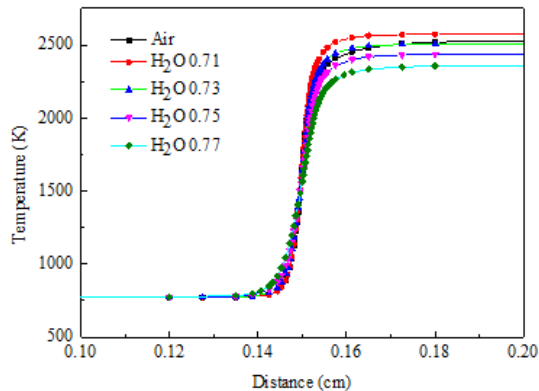


Figure 1. Temperature profiles for the different molar fraction of H_2O .

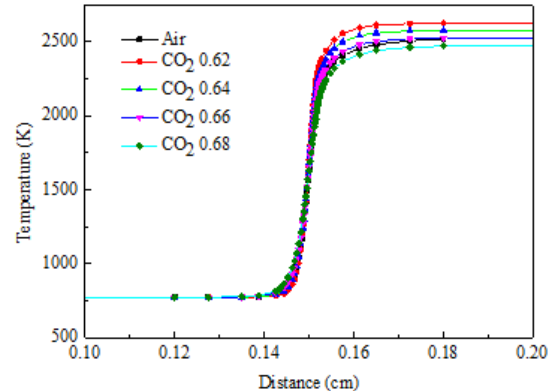


Figure 2. Temperature profiles for the different molar fraction of CO_2 .

While N means the number of the nodes. The temperature derivations for H_2O molar fraction of 0.71, 0.73, 0.75 and 0.77 are 52.74, 32.16, 92.83 and 167.40, respectively. For dilution of CO_2 , the temperature derivation for CO_2 molar fraction of 0.62, 0.64, 0.66 and 0.68 are 97.70, 43.16, 20.81 and 62.27, respectively. Consequently, the temperature profiles of oxyfuel combustion (diluted by H_2O or CO_2) and air-fired condition have the best agreement when the molar fraction of H_2O and CO_2 are 0.73 and 0.66, respectively. Therefore, the following simulation work will focus on the effects of turbulence intensity on these two conditions as shown in table 2.

Table 2. Case arrangement.

Parameters	Case	1	2	3	4	5	6	7	8	9	10	11
Species	CH_4	0.095	0.1	0.180	0.145	0.145	0.145	0.1	0.141	0.119	0.119	0.12
	O_2	0.190	0.190	0.360	0.291	0.291	0.291	0.190	0.282	0.238	0.238	0.24
	N_2	0.715				-	-					
	CO_2		0.715	0.460	0.564	0.564	0.564					
	H_2O							0.715	0.577	0.643	0.643	0.64
u' (m/s)		0.8	0.8	0.8	0.8	1.6	2.4	0.8	0.8	0.8	1.6	2.4
S_L (cm/s)		106	14	148	71	71	71	59	181	115	115	115
δ_L (μm)		50.8	213.0	33.5	57.0	57.0	57.0	108.1	41.1	60.8	60.8	60.8
Re_l		46.2	69.5	60.2	63.9	127.8	191.7	40.2	40	40.4	80.8	121
η (μm)		28.2	20.8	23.1	22.1	13.2	9.7	31.3	31.4	31.2	18.6	13.7
Δx		15.6	15.6	15.6	15.6	7.8	7.8	15.6	15.6	15.6	15.6	7.8

2.2. Initial Condition

Figure 3 shows the initial fields of velocity and temperature. The present 3-D DNS study is investigated with decaying homogenous turbulence in a constant vessel, with the periodic boundary condition for all directions. The size of the vessel is 2 mm X 2 mm X 2 mm. And each side is discretized with $N=128$ or 256 grids point. The homogenous turbulence is generated by the spectral method, and the turbulence integral scale l_0 was set to 0.5 mm such that the computational domain at least has $4l_0$. The Reynolds numbers based on integral scale and the Kolmogorov scale are shown in table 2. For case 5, 6, 11, the mesh scale is $7.8125 \mu\text{m}$ while for other cases it is 15.625 , which is adequate to solve the Kolmogorov scale. Under the typical ICE condition, the flamelets combustion regime is considered in present study, so a weak homogenous turbulence is adopted and u' of the velocity field is 0.8 m/s. In addition, 1.6 and 2.4 m/s are adopted to investigate turbulence intensity effects. The condition of the cylinder at the Top Dead Center (TDC) in conventional spark ignition ICE is adopted as the initial pressure and temperature.

The initial uniform pressure, p_0 , is 1 MPa while the preheat temperature, T_0 , is 773 K. There is a high temperature ignition kernel in the central of the domain, while other area is to preheat mixture which consists of CH_4 , O_2 and dilution agents. T_{ig} , the temperature of the ignition kernel and r_c , the radius of the ignition kernel are 2000 K and 0.2 mm, respectively. The stoichiometric mixture is preferred for all cases due to less wasted energy and more completely combustion.

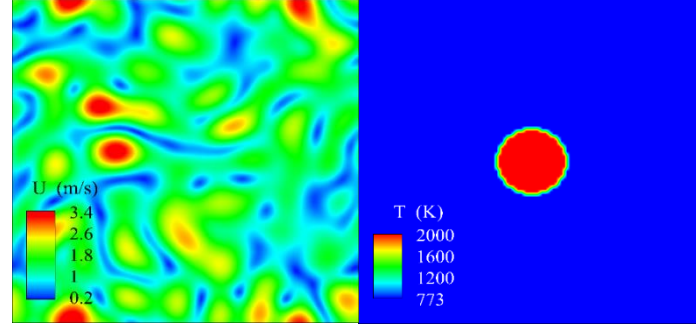


Figure 3. Initial field of (left) velocity with u' 0.8 m/s and (right) temperature for all cases.

2.3. Conservation Equation and Numerical Methods

The mass, momentum, energy and species conservation equations are solved for reacting flow. The viscous heating source term, the Soret and Dufour effects and radiative heat transfer are neglected in this work.

The mass conservation equation is:

$$\frac{\partial \rho}{\partial t} + \nabla \cdot (\rho \vec{v}) = 0 \quad (2)$$

The momentum conservation equation is:

$$\frac{\partial \rho \vec{v}}{\partial t} + \nabla \cdot (\rho \vec{v} \vec{v}) = -\nabla p + \nabla \cdot \vec{\tau} + \rho \vec{g} \quad (3)$$

The energy conservation equation is:

$$\frac{\partial \rho h_s}{\partial t} + \nabla \cdot (\rho \vec{v} h_s) + \frac{\partial \rho K}{\partial t} + \nabla \cdot (\rho \vec{v} K) = \nabla \cdot (\alpha \nabla h_s) + \dot{\omega}_T + \frac{\partial p}{\partial t} + \nabla \cdot (\rho \sum_i^N Y_i V_i h_k) \quad (4)$$

The species conservation equation is:

$$\frac{\partial \rho Y_i}{\partial t} + \nabla \cdot (\rho \vec{v} Y_i) = \nabla \cdot (\rho D_i \nabla Y_i) + \dot{\omega}_i \quad (5)$$

Here Y_i is the mass fraction, K is the turbulent kinetic energy. $\dot{\omega}_T$ is the heat release due to the chemical reactions.

It should be noted that the last term in equation (4) is assumed to zero, because it is typically much smaller than other terms in the equation, according to Giannakopoulos's work [11]. And the diffusion coefficient D_i of the i -th species in mixture is calculated by the Schmidt number which is assumed to 0.7 for all species.

$$\dot{\omega}_T = -\sum_{i=1}^N \Delta h_{f,i}^0 \dot{\omega}_i \quad (6)$$

$$K = \frac{1}{2}(\bar{v})^2 \quad (7)$$

$$D_i = \frac{\mu_i Sc}{\rho_i} \quad (8)$$

The viscosity is calculated using the Sutherland law [12].

$$\mu = \frac{A_s T^{\frac{1}{2}}}{1 + T_s / T} \quad (9)$$

The modeling approach for reacting flow developed in this work is implemented using OpenFOAM[®] finite volume library [13], and is based on the packaged reacting Foam solver. The conservation equations are solved with finite volume method using second order differential schema on mesh, by using PIMPLE algorithm. The detailed CH₄ chemical kinetic mechanism of GRI-mech 3.0 [14] is adopted, which including 53 species and 325 elementary reactions. As it has been validated by the experiment, it has been widely used to simulate methane combustion in oxy-fuel combustion [7,8]. The air-fired condition is considered as a baseline case. For all cases the Co<0.3 is adopted, and the total physical time is 500 μ s.

3. Results and discussion

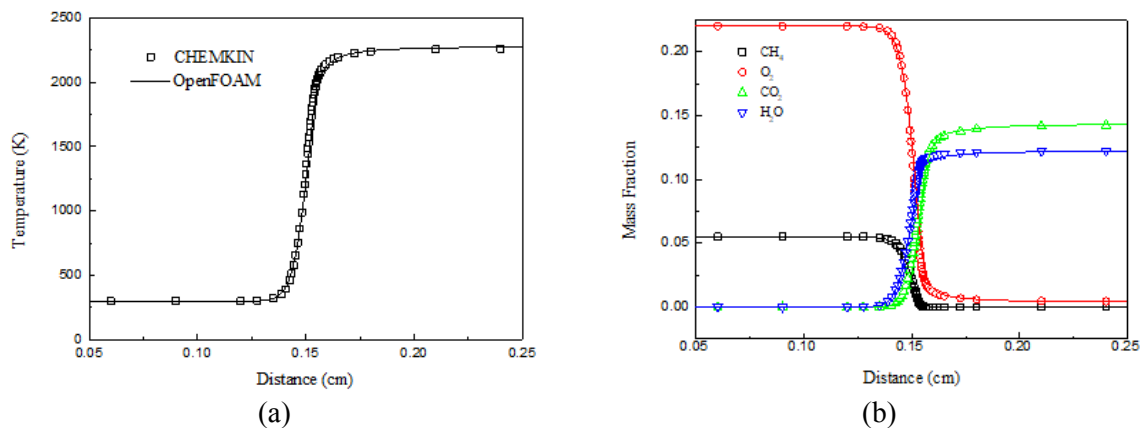


Figure 4. (a) Temperature profiles of OpenFoam and Chemkin on 1D laminar premixed flame and (b) Molar fraction of main species of OpenFoam and Chemkin on 1D laminar premixed flame.

A one-dimensional DNS study of laminar premixed flame is performed. The domain is 3 mm and has 12000 grids point. The results compared to the CHEMKIN laminar premixed flame are shown in figure 4. The profiles of temperature and the mass fraction of the main species have good agreements. Conventionally, about 10 grid points should be within the laminar flame thickness, which can't be afforded in this work since 11 cases are conducted.

3.1. Overall combustion characteristic

Figure 5 shows the temporal development of the mean pressure (p_m) for each case. Combustion at first occurs in the center of the vessel on account of the high temperature, delivering heat and radical to the unburned gas. The flame spreads out as the flame front propagations. It can be observed that p_m has a monotonically increasing phenomenon for all cases. According to figure 5, there is a significant difference between CH₄/O₂/CO₂, CH₄/O₂/H₂O and CH₄/air if N₂ is replaced by equimolar CO₂ or H₂O.

This may be mainly due to the discrepancy of the thermal heat capacity. With the molar fraction of dilution (CO_2 , H_2O) increases the pressure rising rate declines since there are more dilution and less fuel in the vessel. In addition, for CO_2 -66 (the case name means the dilution name- the molar fraction of the dilution in the oxidizer- the value of u' , and the u' default number is 0.8 m/s), H_2O -73 and N_2 -79 the profiles of p_m are diverse, even if they have very closed temperature profiles in laminar premixed flame. This indicates that the flame speed also has a great effect on the application of oxy-fuel combustion in ICE. However, the profile of CO_2 -66-1.6 has a good agreement with N_2 -79. This means that appropriate u' of initial velocity field is important for oxy-fuel combustion to fit in current ICE while it remains a suitable temperature profile. It is also shown in figure 5 that with turbulence intensity increases the pressure rises more rapidly. Both for CO_2 -66 and H_2O -73, the flame surface is wrinkled by the turbulent and higher turbulent intensity. This leads larger flame surface which accelerates flame propagation.

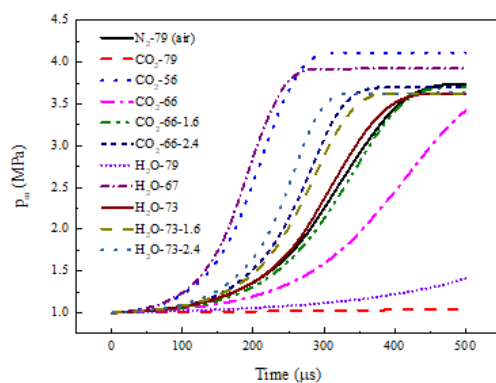


Figure 5. Temporal development of mean pressure in the vessel for different conditions.

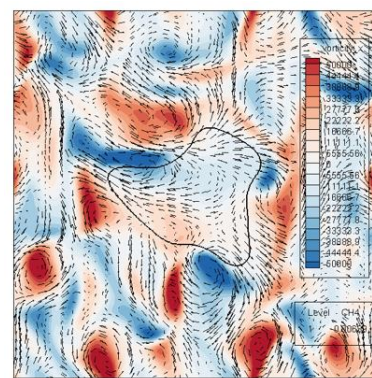


Figure 6. Vorticity effects on flame surface. A central slice of y-z plane. The black line represents the flame surface.

As shown in figure 6, 10% of fuel mass fraction iso-surface is picked as the flame surface, where around the maximum heat release rate in laminar premixed flame. Vorticity x is calculated as $(\partial v_z)/\partial y - (\partial v_y)/\partial z$. The location and intensity of vortex have great effects on the flame surface bending direction. The flame surface stretches along the direction of the vortex. At 50 μs , the area of flame surface of CO_2 -66, CO_2 -66-1.6, CO_2 -66-2.4, H_2O -73, H_2O -73-1.6 and H_2O -73-2.4 are 1.39, 1.62, 2.03, 1.63, 1.82 and 2.16 mm^2 , respectively. The area of flame surface is determined by the laminar flame speed and the initial velocity field. As u' increases, the disparity between CO_2 -66 and H_2O -73 reduces. The evolution of the maximum temperature (max-T) for all cases is shown in figure 7. In the figure 7 the highest temperature of for all cases is 3000 K due to the temperature upper restriction of GRI 3.0. From figure 7, it can be seen that with the molar fraction of dilution (CO_2 , H_2O) decreases max-T rises. It is also shown that the development of max-T is not monotone, which is mainly because at beginning the ignition kernel releases a lot of heat and the temperature is rising rapidly. Then with the flame propagates heat transfers to surrounding gas, and surrounding gas combustion will yield new high temperature gas. For cases of CO_2 -66, CO_2 -66-1.6 and CO_2 -66-2.4 which have a similar decline profiles until 180 μs , the stronger the turbulence is, the earlier and higher the max-Y goes up during flame propagation. This may be resulted from the turbulence which can enhance heat and gas exchange between burnt side and unburnt side. The same phenomenon can be observed between H_2O -73, H_2O -73-1.6 and H_2O -73-2.4. Moreover, comparing cases of H_2O -73, CO_2 -66 and N_2 -79 with the same u' initial velocity field and closed laminar premixed flame temperature profiles, the difference of max-T between those cases can be up to 200 K during flame propagation. This suggests that, under the pressure rising condition, the interaction between turbulence and chemistry has a great effect on oxy-fuel combustion. As shown in figure 8, heat release rate is normalized by the maximum heat release rate during 500 μs after ignition. Except cases of CO_2 -79, H_2O -79 and CO_2 -66, fuel in other cases has run

out. They all get the maximum heat release rate when the pressure is approaching the constant value.

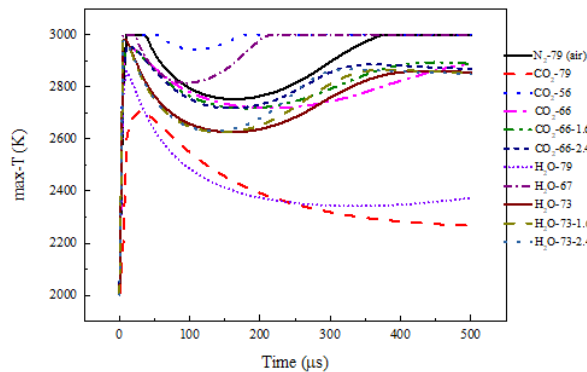


Figure 7. Temporal development of maximum temperature in the vessel for different conditions.

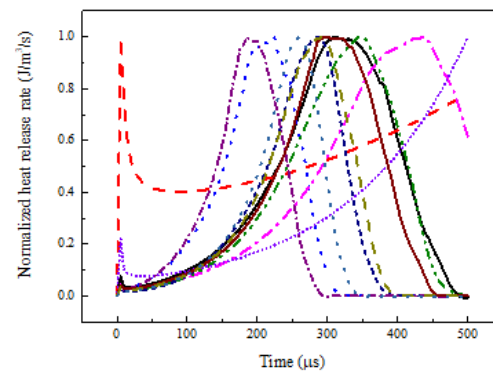
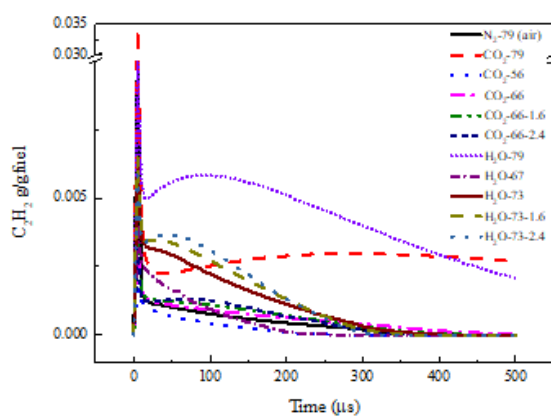


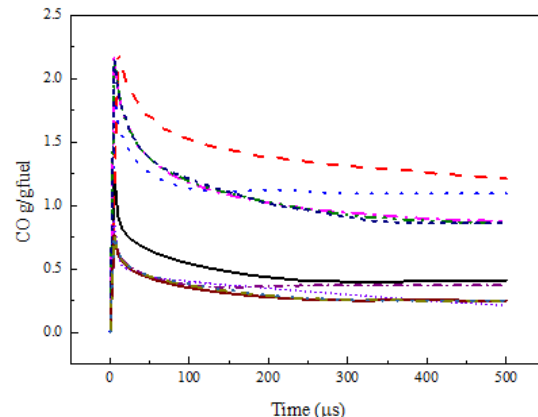
Figure 8. Temporal development of normalized heat release rate in the vessel for different conditions.

3.2. Emissions

As NO_x emissions are neglected in oxy-fuel combustion due to nitrogen's absence, emissions mainly consist of hydrocarbon (HC) and carbon monoxide (CO). As C_2H_2 is considered as the precursor to the soot in ICE, reducing C_2H_2 during flame propagation is very meaningful. Figure 9 shows the evolution of the total mass of C_2H_2 and CO per gram of fuel along with the flame front spreading. After ignition, the masses of C_2H_2 and CO both have a rapid decrease. Cases of CO_2 -79 and H_2O -79 yield more C_2H_2 and CO due to the lower flame temperature and flame speed. Generally, C_2H_2 decreases to zero gradually with the consuming of CH_4 while CO keeps to a constant level finally. It should be noticed that the mass of C_2H_2 of oxy- H_2O is higher than oxy- CO_2 , and higher turbulent intensity will bring about higher C_2H_2 at the beginning of flame propagation. In terms of CO, it is shown turbulence intensity has little effect on the formation of CO, and the mass of CO rises in the first stage then decreases with the increases of the mole fraction of dilution (H_2O and CO_2). For the case of CO_2 -79, the generation of CO is mainly because of low flame temperature. But as for the case of CO_2 -56, the dissociation of CO_2 under high temperature with the reaction of $\text{CO}_2 + \text{H} = \text{CO} + \text{OH}$ is the major way to produce CO. This is also the reason why oxy- CO_2 produces more CO than oxy- H_2O under the same dilution mole fraction. From the view point of emission control, H_2O is the better dilution than CO_2 . The total masses of C_2H_2 and CO under air-fired condition are kept at a low level compared to oxy-fuel combustion, though the formation of NO_x in air-fired combustion is inevitable.



(a)



(b)

Figure 9. (a) Temporal development of the mass of C₂H₂ per mass of consumed fuel in the vessel for different conditions and (b) Temporal development of the mass of CO per mass of consumed fuel in the vessel for different conditions.

3.3. Flame displacement speed

For most premixed propagation combustion, the motion of the flame is characterized by the Flame Displacement Speed (FDS), which is defined as the speed of the flame surface relative to the fresh gas. It has been found that the value of FDS is insensitive to the reference position of the flame front within the flame in flamelets combustion model [11]. And the flame displacement speed, S_d , is calculated by [15]:

$$S_d = -\frac{1}{\rho |\nabla Y_{CH_4}|} [\nabla D_{CH_4} (\nabla Y_{CH_4}) + \dot{\omega}] \quad (10)$$

For a meaningful comparison with the laminar flame speed, the density-weighted flame displacement speed (S_d^*) is calculated as:

$$S_d^* = \frac{\rho_b}{\rho_u} S_d \quad (11)$$

Here ρ_b is the density of the burnt gas, while ρ_u is the density of the unburnt gas.

For convenience, the maximum and minimum of the density are adopted as the ρ_b and ρ_u respectively. In the constant volume vessel, the pressure increases with the flame propagations, and the temperature of unburned side increases, which has a significant effect on the process of the combustion. Therefore, in order to obtain the corresponding S_L , premixed laminar flame is conducted by adopting minimum temperature and mean pressure in the vessel as the inlet condition in CHEMKIN. The mean displacement flame speed $\overline{S_d^*}$ of flame surface is studied with pressure rising condition. Furthermore, the local S_d^* is investigated using Probability Density Function (PDF) method. The characteristic of the flame displacement speed is investigated under the pressure of 1.5, 2.25 and 3 MPa, and cases of CO₂-79 and H₂O-79 are neglected due to poor condition of combustion. Figure 10 shows the change of $\overline{S_d^*}/S_L$ under 1.5, 2.25 and 3 MPa, with the increment of pressure the value of $\overline{S_d^*}/S_L$ is rising. Oxy-CO₂ rise faster in the second stage than the first stage, while oxy-H₂O has an opposite phenomenon, which means oxy-CO₂ combustion is more sensitive to the pressure rising condition. Comparing cases of CO₂-66, CO₂-66-1.6 and CO₂-66-2.4, the value of $\overline{S_d^*}/S_L$ is higher when the u' is bigger. The same phenomenon is also observed in oxy-H₂O condition. As PDF analysis is present in figure 11, the peak value of the probability is around 1.0 for all cases, because in flamelets combustion mode local flame combustion is under laminar flame condition.

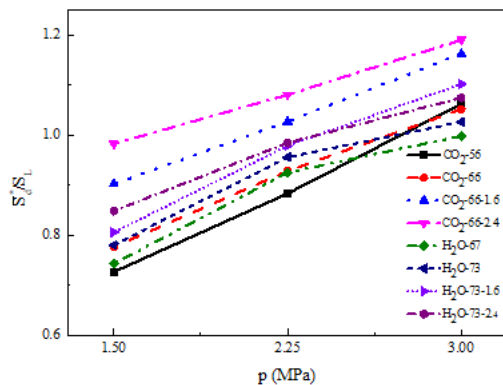


Figure 10. Ratio of the mean flame displacement speed of the flame surface and laminar flame speed under 1.5, 2.25 and 3 MPa.

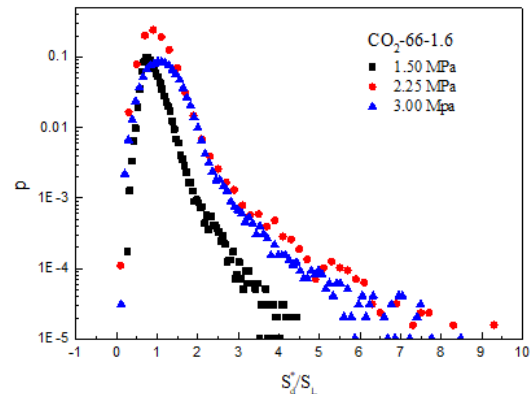


Figure 11. PDF analysis of local flame displacement speed for different conditions.

4. Conclusions

This work presents an investigation on turbulent premixed oxy-fuel combustion with different dilution agents, molar fraction of dilution and turbulent intensity.

- A 3D DNS numerical study with detail chemistry mechanism has been conducted to examine turbulent premixed combustion with oxyfuel mixtures under similar operating conditions as happened in spark ignition Internal Combustion Engine (ICE). H₂O and CO₂ are adopted as the dilution in oxy-fuel combustion.
- The temperature profiles of oxy-H₂O and oxy-CO₂ combustion are consistent with those of air-fired conditions in laminar premixed flame when the molar fraction of H₂O and CO₂ are 73% and 66% in oxidizer, respectively.
- 79%, 67% molar fraction of H₂O and 79%, 56% molar fraction of CO₂ are also conducted to learn the effects of the dilution molar fraction on the process of flame propagation.
- With the molar fraction of dilution increases, the mass of C₂H₂ increases the flame propagation speed and the mass of CO does an opposite influence.
- With the investigation for effects of turbulent intensity under conditions of 73% H₂O and 66% CO₂ with the initial u' of 0.8, 1.6 and 2.4 m/s, respectively, results show that the turbulent intensity has little effect on the formation of CO.
- It is also demonstrated that for oxy-fuel combustion, due to the disparity in laminar flame speed, an appropriate u' is necessary to keep consistent with the flame propagation speed meanwhile to maintain suitable temperature profiles.

Acknowledgments

Financial supports from the ERDF (European Regional Development Fund) (Interreg NEW 553 - RIVER) are gratefully acknowledged.

References

- [1] Mletzko J, Ehlers S and Kather A 2016 Comparison of natural gas combined cycle Power plants with post combustion and oxyfuel technology at different CO₂ capture rates *Energy Procedia* **86** 2-11
- [2] Liaw S B, Chen X J, Yu Y, Costa M and Wu H W 2018 Effect of particle size on particulate matter emissions during biosolid char combustion under air and oxyfuel conditions *Fuel* **232** 251-6
- [3] Mohammad R S, Yinka S S and Esmail M A M 2018 Numerical modeling of oxy-methane combustion in a model gas turbine combustor *Appl. Energy* **228** 68-81
- [4] Li H, Yan J, Yan J and Anheden M 2009 Impurity impacts on the purification process on oxy-

- fuel combustion based CO₂ capture and storage system *Appl. Energy* **86** 202-13
- [5] Liu C Y, Chen G, Sipöcz N, *et al* 2012 Characteristics of oxy-fuel combustion in gas turbines *Appl. Energy* **89** 387-94
- [6] Krieger G C, Campos A P V, Takehara M D B, *et al* 2015 Numerical simulation of oxy-fuel combustion for gas turbine applications *Appl. Therm. Engin.* **78** 471-81
- [7] Zou C, Song Y, Li G, *et al* 2014 The chemical mechanism of steam's effect on the temperature in methane oxy-steam combustion *International J. Heat & Mass Transfer* **75** 12-8
- [8] Song Y, Zou C, He Y, *et al* 2015 The chemical mechanism of the effect of CO₂, on the temperature in methane oxy-fuel combustion *Int. J. Heat & Mass Tran.* **86** 622-8
- [9] Mazas A N, Fiorina B, Lacoste D A, *et al* 2011 Effects of water vapor addition on the laminar burning velocity of oxygen-enriched methane flames *Combust. Flame* **158** 2428-40
- [10] Yang Z, Yu X, Peng J, *et al* 2017 Effects of N₂, CO₂, and H₂O dilutions on temperature and concentration fields of OH in methane Bunsen flames by using PLIF thermometry and bi-directional PLIF *Exp. Therm. Fluid Sci.* **81** 209-22
- [11] Giannakopoulos G K, Gatzoulis A, Frouzakis C E, *et al* 2015 Consistent definitions of “flame displacement speed” and “markstein length” for premixed flame propagation *Combust. Flame* **162** 1249-64
- [12] Sutherland W 1893 The viscosity of gases and molecular force *Philos. Mag.* **36** 507-31
- [13] Weller H G, Tabor G, Jasak H, *et al* 1998 A tensorial approach to computational continuum mechanics using object-oriented techniques *Computers in Physics* **12** 620-31
- [14] Smith G P, *et al* http://www.me.berkeley.edu/gri_mech/
- [15] Echehki T and Chen J H 1996 Unsteady strain rate and curvature effects in turbulent premixed methane-air flames *Combust. Flame* **106** 184-90